



Structure Report

The structure of AAVrh32.33, a novel gene delivery vector



Kyle Mikals^a, Hyun-Joo Nam^{a,1}, Kim Van Vliet^a, Luk H. Vandenberghe^{b,2}, Lauren E. Mays^b, Robert McKenna^a, James M. Wilson^b, Mavis Agbandje-McKenna^{a,*}

^a Department of Biochemistry and Molecular Biology, Center for Structural Biology, The McKnight Brain Institute, University of Florida, Gainesville, FL, USA

^b Gene Therapy Program, Department of Pathology and Laboratory Medicine, University of Pennsylvania, Philadelphia, PA, USA

ARTICLE INFO

Article history:

Received 12 December 2013

Received in revised form 23 March 2014

Accepted 25 March 2014

Available online 2 April 2014

Keywords:

AAVrh32.33

X-ray crystallography

Parvovirus

Gene therapy

Adeno-associated virus

Virus capsid structure

ABSTRACT

The Adeno-associated viruses (AAVs) are being developed as gene delivery vectors for therapeutic clinical applications. However, the host antibody immune response directed against their capsid, prevalent in ~40–70% of the general population, depending on serotype, negatively impacts efficacy. AAVrh32.33, a novel vector developed from rhesus macaques isolates, has significantly lower seroprevalence in human populations compared to AAV2 and AAV8, which are both in clinical use. To better understand the capsid determinants of this differential immune response to AAVrh32.33, its structure was determined by X-ray crystallography to 3.5 Å resolution. The capsid viral protein (VP) structure conserves the eight-stranded β-barrel core and αA helix reported for other parvoviruses and the distinct capsid surface topology of the AAVs: a depression at the icosahedral twofold axis, three protrusions surrounding the threefold axis, and a depression surround a cylindrical channel at the fivefold axis. A comparison to AAV2, AAV4, and AAV8, to which AAVrh32.33 shares ~61%, ~81%, and ~63% identity, respectively, identified differences in previously defined AAV VP structurally variable regions (VR-1 to VR-IX) which function as receptor attachment, transduction efficiency, and/or antigenic determinants. This structure thus provides a 3D platform for capsid engineering in ongoing efforts to develop AAVrh32.33, as well as other AAV serotypes, for tissue targeted gene-therapy applications with vectors that can evade pre-existing antibody responses against the capsid. These features are required for full clinical realization of the promising AAV gene delivery system.

© 2014 Elsevier Inc. All rights reserved.

1. Introduction

Adeno-associated viruses (AAVs) hold great promise as clinical gene delivery vectors due to their lack of pathogenicity and ability to deliver packaged foreign genes for high levels of protein expression in different human tissues (Gao et al., 2005). Several AAV serotypes, including AAV1, AAV2, and AAV8, have been used in human clinical trials (Maguire et al., 2009; Mingozi and High, 2011a; Nathwani et al., 2011). However, the host antibody immune response to the AAVs, which is detrimental to therapeutic efficacy, is prevalent in a large portion percent (~40–70%) of the general population (Asokan et al., 2012; Boutin et al., 2010; Calcedo et al., 2009; Mingozi and High, 2011a,b; Nathwani et al., 2011).

These antibodies neutralize AAV vectors in a serotype-specific manner. Thus significant effort is being extended to identify AAV vectors with a low immune prevalence in the human population and to understanding the antigenic structure of the capsid epitopes towards elucidating the epitopes to which these responses are directed (Gurda et al., 2012, 2013; Huttner et al., 2003; Lochrie et al., 2006; Maheshri et al., 2006; McCraw et al., 2012; Moskalenko et al., 2000; Perabo et al., 2006; Wobus et al., 2000).

A worldwide epidemiology study demonstrated that AAVrh32.33, a hybrid of two rhesus macaque isolates, AAVrh32 and AAVrh33 (Lin et al., 2009; Vandenberghe et al., 2009), had significantly lower seroprevalence than AAV1, AAV2, AAV7, and AAV8 in the human population. The natural antibody titers for IgG in response to AAVrh32.33 were reported to be 1:20 while the titers for AAV2 and AAV8 were 1:2560 and 1:320, respectively (Calcedo et al., 2009). AAV4, a serotype that is one of the most structurally and serologically different from other human and non-human primate AAVs (Gao et al., 2004; Govindasamy et al., 2006) but shares high (~81%) sequence similarity with AAVrh32.33, was found to have a similar low antibody response (Calcedo et al., 2009). Thus AAVrh32.33 (and AAV4) are attractive for development as a gene

* Corresponding author. Address: 1600 SW Archer Road, Gainesville, FL 32610, USA.

E-mail address: mckenna@ufl.edu (M. Agbandje-McKenna).

¹ Current address: Department of Bioengineering, University of Texas at Dallas, Richardson, TX, USA.

² Current address: Schepens Eye Research Institute, Massachusetts Eye and Ear Infirmary and Harvard Medical School, Boston, MA, USA.

delivery vectors with the potential to evade pre-existing host antibody responses against AAV capsids (Calcedo et al., 2009; Li et al., 2012; Mays and Wilson, 2009; Mays et al., 2009). AAVrh32.33 is also being evaluated as a genetic vaccine platform, specifically for human immunodeficiency virus type 1 (HIV-1) and type A influenza virus (Lin et al., 2009). In mouse models, a robust CD8+ T-cell response to the HIV gag protein expressed from genes delivered with an AAVrh32.33 vector was observed. Studies in macaques, using vectors expressing gp140 from HIV-1, also reported a robust CD8+ T-cell response to gp140 and high titer neutralizing antibodies to HIV-1 (Lin et al., 2009). These studies thus identify AAVrh32.33 as a vector that enables the stimulation of immune responses to expressed transgenes. Interestingly, a comparative study of AAVrh32.33 and AAV8, another non-human primate serotype, showed that the latter induces a minimal CD8+ T-cell response (Mays et al., 2009). The AAV capsid is reported to play a major role in this phenotype (Mays et al., 2013).

AAVrh32.33, like other AAVs, belongs to the *Dependovirus* genus of the *Parvoviridae* family. These are non-enveloped viruses which package their 4.7 kb ssDNA genomes into capsids which are ~260 Å in diameter and have $T = 1$ icosahedral symmetry. The capsid is assembled from 60 copies of a combination of three overlapping viral proteins (VPs), VP1, VP2, and VP3, encoded from the *cap* open reading frame of their genome. VP1 is the largest VP at ~81 kDa, has a unique N-terminal region (VP1u) of 137 amino acids, and contains the entire sequence of VP2. VP3, the major capsid protein, is ~60 kDa and contained within VP2 which has an additional 65 amino acids (VP1/2 common region) compared to VP3. The predicted capsid ratio of VP1:VP2:VP3 is 1:1:10 (Buller and Rose, 1978; Johnson et al., 1971; Rose et al., 1971).

The 3D structure of several AAV serotypes have been determined by X-ray crystallography and/or cryo-electron microscopy and image reconstruction (DiMattia et al., 2012; Govindasamy et al., 2006, 2013; Lerch et al., 2010; Nam et al., 2007; Ng et al., 2010; Padron et al., 2005; Xie et al., 2011, 2002). In all these structures, only the VP3 overlapping region has been clearly resolved in electron density maps (Chapman and Agbandje-Mckenna, 2006; Halder et al., 2012). This VP3 structure contains a conserved

eight-stranded anti-parallel β -barrel (designated β B- β I) plus β -strand A (β A) that forms the contiguous capsid shell, α helix (α A), and large loops inserted between the β -strands. The loops, which form the majority of the capsid surface, contain small stretches of β -strand structure, and variable regions (VRs) at their apex, designated VR-I to VR-IX, based on the comparison of AAV2 and AAV4 (Govindasamy et al., 2006). The sequence and structure variation in the VRs serve as determinants of differential receptor attachment, transduction efficiency, and antigenicity between the AAVs (DiMattia et al., 2012; Govindasamy et al., 2006; Gurda et al., 2012, 2013; McCraw et al., 2012; Nam et al., 2007; Ng et al., 2010; Xie et al., 2011). Conserved capsid surface features, formed by the interaction between symmetry related VP3 monomers, are depressions at the icosahedral twofold symmetry axis and surrounding the fivefold axis, protrusions surrounding the threefold axes, and a cylindrical channel at the fivefold axis.

Reported here is the structure of AAVrh32.33 determined to 3.5 Å by X-ray crystallography. To better understand the capsid determinants of its differential immune response properties, the structure was compared to those of AAV2, AAV4, and AAV8 to which AAVrh32.33 shares ~61%, ~81%, and ~63% identity, respectively. As with the other AAV structures, only the VP3 common region of AAVrh32.33 is ordered and it conserves the VP topology and surface features described above. Comparison of AAVrh32.33 to the other AAVs showed high similarity to AAV4, with smaller structural variations observed between their VR-I to VR-IX compared to AAV2 and AAV8. This structure thus identifies AAV capsid surface features that can drive ongoing efforts to develop AAVrh32.33, as well as other AAV serotypes, for tissue targeted gene-therapy applications. In addition, it provides information on regions that can be modified to generate vectors capable of evading pre-existing antibody responses against the capsid for improved therapeutic efficacy.

Table 1
Crystal data-collection and processing statistics.

Parameter	Value
Resolution (Å)	40–3.5 (3.63–3.5)
Space group/crystal system	P1
Unit cell (Å, °)	$a = 246.4$, $b = 247.5$, $c = 250.3$, $\alpha = 70.4$, $\beta = 65.4$, $\gamma = 60.2$
R_{merge}^a	0.16 (0.39)
Completeness (%)	68.5 (66.0)
I/σ	2.98 (1.65)
R_{factor}^b	0.28
R_{free}^c	0.28
No. of observed reflections	727,358
No. of unique reflections	397,503
No. of protein atoms	4117
RMSD for bond lengths (Å)	0.014
RMSD for bond angles (°)	1.82
Avg B factor, main chain (Å ²)	41.1
Avg B factor, side chain (Å ²)	41.4
Avg B factor, NT (Å ²)	55.8
Residues in the most/additional/ generously allowed regions (%)	88.5/11.5/0

^a Calculated as $\Sigma |I_{hkl} - \langle I_{hkl} \rangle| / \langle I_{hkl} \rangle$, where I_{hkl} is a single value of the measured intensity of the hkl reflection and $\langle I_{hkl} \rangle$ is the mean of all measured values of the intensity of the hkl reflections.

^b Calculated as $\Sigma ||F_o| - |F_c|| / |F_o|$, where F_o and F_c are the observed and calculated structure factors, respectively.

^c Same as R_{factor} , but calculated with a 5% randomly selected fraction of the reflection data not included in the refinement.

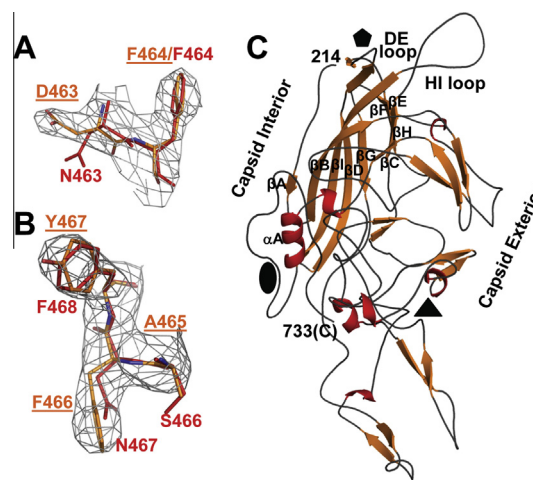


Fig. 1. Structure of AAVrh32.33. (A, B) Section of the $2F_o - F_c$ electron density map (gray mesh) for residues 463–467 contoured at a threshold of 1σ for residues that differ between AAVrh32.33 and AAV4. The AAVrh32.33 residues are colored according to atom type: C – orange, N – blue, O – red; the AAV4 residues are in red in stick form. AAVrh32.33 residue labels are underlined. (C) A ribbon diagram of the AAVrh32.33 VP3 monomer. β -Strand regions are shown as orange ribbons, helical regions are in red and loop regions are in black. The core eight-stranded β -barrel formed by the β BIDG and β CHEF sheets, conserved α A, the DE loop between β D and β E, and the HI loop (between β H and β I), the first N-terminal residue observed (214) and the C-terminal residue (733) are labeled. The sides of the VP monomer forming the capsid interior and exterior surfaces are also labeled. The approximate icosahedral two, three, and fivefold axes are indicated by the filled oval, triangle, and pentagons, respectively. These images were generated with the program PyMOL (<http://www.pymol.org>). (For interpretation of the references to color in this figure legend, the reader is referred to the web version of this article.)

Download English Version:

<https://daneshyari.com/en/article/5914186>

Download Persian Version:

<https://daneshyari.com/article/5914186>

[Daneshyari.com](https://daneshyari.com)